2008 IEEE International Conference on
Robotics and Automation
Pasadena, CA, USA, May 19-23, 2008

Expanding the Twin Pulse Swing Free Profile *

David Bowling, Gregory Starr, John Wood and Ron Lumia
Department of Mechanical Engineering
The University of New Mexico, Albuquerque, New Mexico 87131, USA
(dbowling,starr,jw,lumia)@unm.edu

***Abstract*—The twin-pulse motion profile is still perhaps the simplest profile in existence for reducing residual vibration. Its primary drawback is that of narrow bandwidth, i.e., it is effective for attenuating only a very narrow range of frequencies about its design frequency. This has led to the inclusion of more pulses to improve robustness to frequency variation. However, one cost of adding pulses is extending the duration of the resulting motion. This paper presents several techniques whereby the basic twin-pulse motion profile can be expanded to reduce its frequency sensitivity while still preserving its advantages. These techniques include intentionally mis-aligning the null points of ideal twin pulses and a convolved boxcar function, then adding a trapezoidal profile component, finally culminating in what we term a misaligned boxcar / trapezoidal / twin pulse (M-BC:TZ:TP) motion profile. This expanded profile and a basic twin-pulse profile were both evaluated on a ten-pendula system with natural frequencies varying over a range of nearly 10%. Simulation results showed an overall reduction of 97% with the expanded twin-pulse profile, and notably all ten frequencies were attenuated; only one frequency was attenuated with the standard twin-pulse profile. Experiments using a linear rail transport system and the ten pendula device validated the simulation. These expanded profiles retain the simplicity and short duration of the twin-pulse with increased robustness to frequency variations.**

I. Introduction

Posicast control was the first use of pulses to eliminate unwanted oscillations in lightly-damped systems [1], [2], and was originally developed as a compensator to be used in conjunction with an existing control system. The use of posicast control was then expanded by Starr [3] to the realm of profile generation to create profiles that eliminated or reduced unwanted residual vibrations. Singhose, Singer and Seering [9], [13] expanded Starr's motion work by introducing the concept of input-shaping in which a base profile is convolved with a series of two to five pulses. Both approaches create profiles that first excite then cancel out a range of frequencies in the system that is being driven. Starr's original work solved the problem by ramping up the velocity in two steps, separated by half the period of the natural frequency of the system. Singer and Seering approached the problem by convolving a twin pulse kernel with a position profile. Their pulses were also separated by half the period of the natural frequency of the system. This reduces to Starr's work, since the derivative or velocity of a convolved twin pulse is a two step velocity profile as used by Starr.

The twin-pulse (TP) motion profile used by Starr was sensitive to errors in the natural frequency of the driven system. Convolution based TP input-shaping (IS) reduced the sensitivity to frequency errors and allowed for multiple modes by increasing the number of pulses. The current maximum number of pulses used by Seering, Singer, and Singhose is five as used in the three-hump extra insensitive (EI) shaped motion.

This paper presents a general approach of decreasing the sensitivity of the original TP motion by manipulating the shape and width of the pulses in the classic TP profile.

II. Overview of Existing Pulse-Based profiles

Profiles convolved with a series of pulses can create motion that will not result in residual vibration in a driven system (Figure 1). Actually, pulse-based profiles first introduce vibrations into a system, then cancel out the vibrations when the final series of pulses is applied. Figure 2 shows a series of frequency spectra produced by a three-hump EI shaper. The figure shows the resulting spectra as successive pulses in an EI shaper are applied to a system. The first pulse creates a flat spectrum that excites all frequencies. As each additional pulse is added, the width of the notch increases and the magnitude of the spectrum decreases. If this pulse train is convolved with a step in position, a profile is generated that will cancel out all residual vibration over a given frequency range. This is the basic implementation of TP and IS motion (from a signal processing view) as first described by Starr (Figure 1).

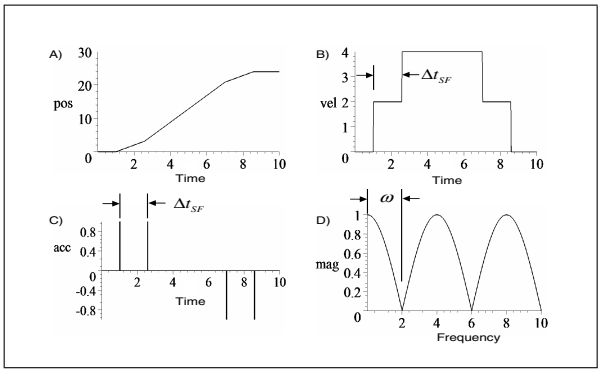

Fig. 1: *Swing Free motion with $\Delta t_{SF} = \pi/\omega$. A) Position profile; B) Velocity profile; C) Acceleration profile; D) Frequency spectrum with null point at $\omega =$ 2 rad/sec.*

*This work is supported by DOE Grant #DE-FG52-04NA25590 awarded to the UNM Manufacturing Engineering Program

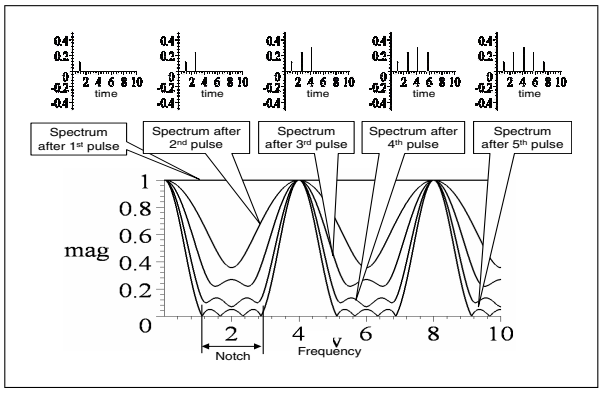

Fig. 2: *Input Shaping excites a system with its first pulse. As each successive pulse is applied to the system, the frequency spectrum magnitude is reduced and the notch widens.*

III. Minimal Pulse-Based Profiles

A. Twin Pulse (TP) Profile

Starr's original work was based on exciting and then canceling the energy in a system using two pulses. However, a pulse (Dirac function) cannot be physically realized in software or hardware. The pulses must have some physical width, usually limited by the frequency or sampling period of software and hardware. When width is added to the pulses, the shape of the frequency response of the TP profile starts to change. The frequency spectrum of the original TP motion and the shape of the pulse itself are multiplied together to create a final combined frequency spectrum.

B. Twin Pulse / Boxcar Motion Profiles (TP:BC profile)

This combining of the spectra can be advantageous. If the points in the frequency spectrum where the magnitude goes to zero (null or notch frequency) are aligned, the overall sensitivity of the profiles can be reduced. For example, if boxcar functions are used for the pulses, the null points can be aligned to decrease the sensitivity (or increase the effective width) of the notch in the frequency domain. Thus the slope of the spectrum at the notch is reduced at the center frequency (Figures 3, 4).

When designing a standard twin pulse profile the desired frequency to be canceled, ω_n, is aligned with the first null frequency of the profile. The profile in Figure 3 has the desired cancellation frequency aligned with the second null point of the TP spectrum. The frequency spectrum of the $TP : BC$ profile is given by,

$$mag_{(TP:BC)} = \frac{1}{4\omega\pi}\left|e^{\left(\frac{(-2k-1)j\pi\omega}{\omega_n}\right)} - e^{\left(\frac{(-2k+1)j\pi\omega}{\omega_n}\right)} + e^{\left(\frac{-2j\pi\omega}{\omega_n}\right)} - 1\right|, \quad (1)$$

where

k = The twin pulse null point number to align with the boxcar null point

ω_n = Notch frequency

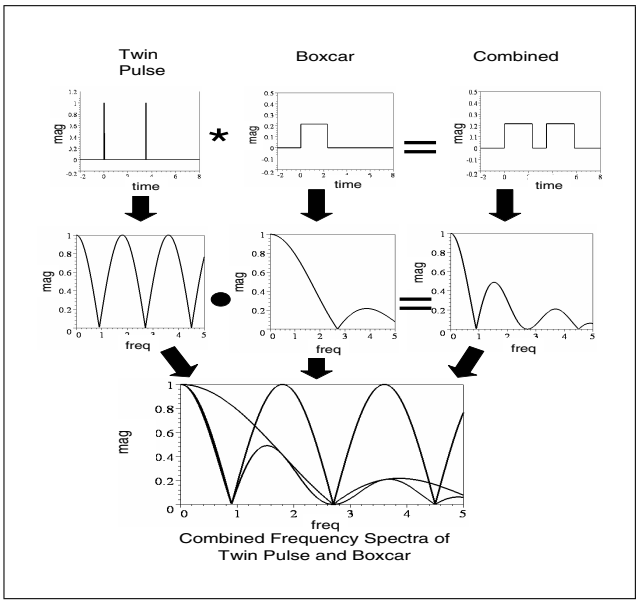

Fig. 3: *Result of combining a twin pulse (TP) with a boxcar (TP:BC)when null points are aligned. The second null point ($k = 2$) is aligned with the boxcar null point.*

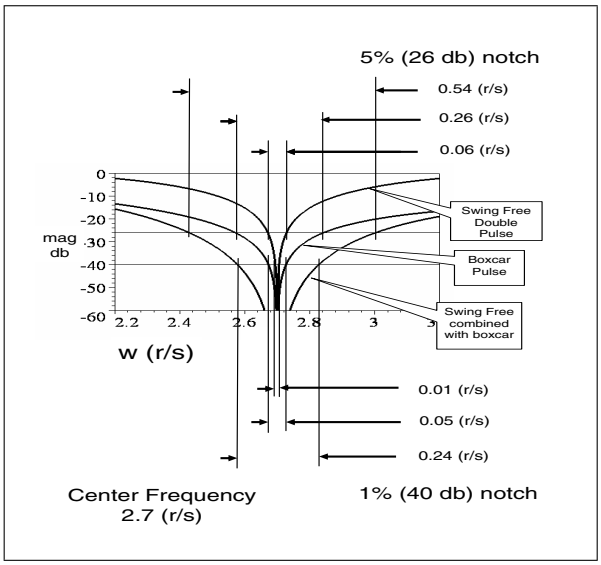

Fig. 4: *Close up Semi-log plot of combined twin pulse with a boxcar (TP:BC) of Figure 3.*

The width Δt of the boxcar, and the space between the two pulses of the $TP : BC$ profile are given by (2) and (3):

$$\Delta t_{\text{boxcar(TP:BC)}} = \frac{2\pi}{\omega_n} \quad (2)$$

$$t_{\text{interpulse(TP:BC)}} = \frac{\pi}{\omega_n}(2k-1). \quad (3)$$

The total time required for the profile (length of the kernel) is the sum of equations (2) and (3):

$$\Delta t_{\text{kernel(TP:BC)}} = \frac{\pi}{\omega_n}(2k+1). \quad (4)$$

For the first null point of a twin pulse and boxcar function to align, the width of the boxcar must be twice the distance between the pulses. This creates an FIR filter (kernel) with a pyramid shape (Figure 5). This kernel profile closely resembles the first improvements of Singer and Seering IS, with three pulses.

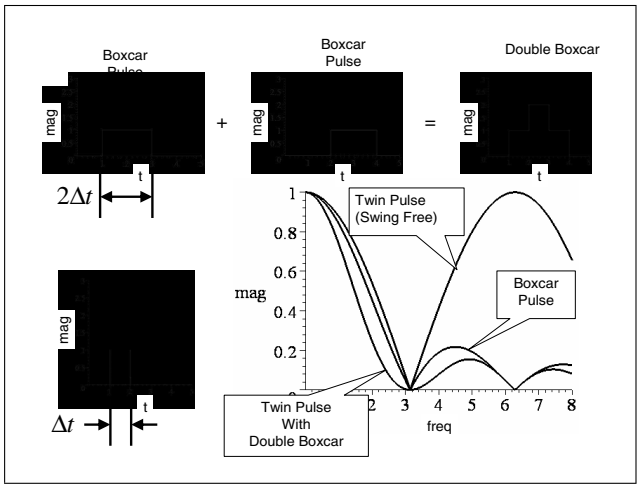

Fig. 5: *Result of combining a twin pulse of width = Δt_{TP} and a boxcar of width = $\Delta t_{BC} = 2\Delta t_{TP}$.*

C. Mis-aligned Twin-Pulse / Boxcar Profiles (M-TP:BC profiles)

The notch width of the Twin Pulse / Boxcar motion profile can be increased further by slightly mis-aligning the null points of the twin pulse and the boxcar (Figure 6). The null points of the boxcar and twin pulse can be slightly offset by $\delta\omega_n$ on each side of the desired notch frequency ω_n. The frequency spectrum of the offset profile is defined by equation (5). Given a desired error for the frequency spectrum magnitude, the corresponding offset $\delta\omega_n$ can be found by iterating over (5) using an algorithm such as the bisection method [25].

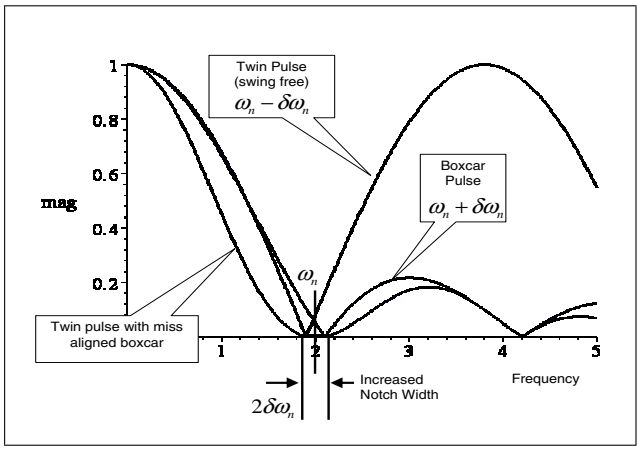

Fig. 6: *Combining a twin pulse with small mis aligned boxcar to increase frequency notch (M-TP:BC).*

$$mag_{(M-TP:BC)} = \frac{1}{4\omega\pi}\left|j\left(\omega_n+\delta\omega_n\right)\left(e^{\left(\frac{-j\pi\omega}{\delta\omega_n-\omega_n}\right)}+1\right)\left(e^{\left(\frac{-2j\pi\omega}{\omega_n+\delta\omega_n}\right)}-1\right)\right| \quad (5)$$

It should be noted that the offset $\delta\omega_n$ can be added to the boxcar ω_n and subtracted from the twin pulse ω_n (referred to as the $M-TP:BC$ method) or subtracted from the boxcar and added to the twin pulse (referred to as the $M-BC:TP$ method). If the latter method is chosen, the frequency spectrum of (6) is created.

$$mag_{(M-BC:TP)} = \frac{1}{4\omega\pi}\left|j\left(\omega_n-\delta\omega_n\right)\left(e^{\left(\frac{-j\pi\omega}{\omega_n+\delta\omega_n}\right)}+1\right)\left(e^{\left(\frac{-2j\pi\omega}{\omega_n+\delta\omega_n}\right)}-1\right)\right| \quad (6)$$

The length of the kernel is also affected by the method. The $M-TP:BC$ method creates the shortest kernel but has a larger magnitude, resulting in higher acceleration. The length of both kernels is shown in equations (7) and (8). The shape of the kernel for the $M-TP:BC$ profile is shown in Figure 7. The primary difference between the methods is the order in in which the null points appear in the frequency domain. For the $M-TP:BC$ the twin pulse null point has the lower frequency.

$$\Delta t_{\text{kernel(M-TP:BC)}} = \frac{\pi(3\omega_n - \delta\omega_n)}{\omega_n^2 - \delta\omega_n^2} \quad (7)$$

$$\Delta t_{\text{kernel(M-BC:TP)}} = \frac{\pi(3\omega_n + \delta\omega_n)}{\omega_n^2 - \delta\omega_n^2} \quad (8)$$

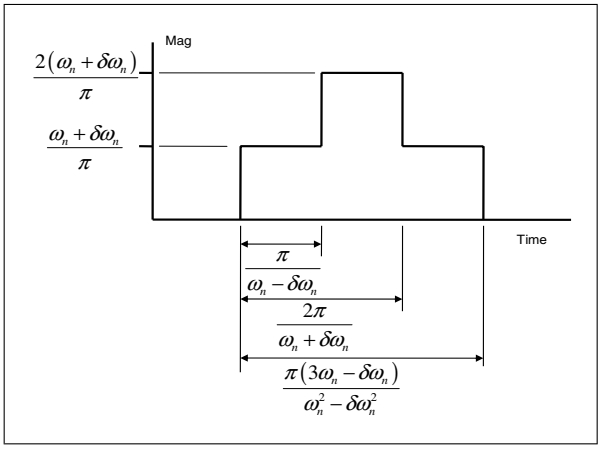

Fig. 7: *Kernel shape for a mis-aligned (M-TP:BC) profile*

D. Boxcar / Velocity Ramp (BC:VR) Motion Profile

If we let the width of the boxcar functions and the twin pulse be equal in length they combine to form a single boxcar function with a length twice that of the twin pulse. This is a straightforward pulse-based profile. A simple boxcar can create the same null point effect in the frequency domain, but

also has the same robustness issues (but not quite as severe) as the twin pulse profile. The advantage of the twin pulse is that the duration of the kernel can be less than that of a boxcar. If the magnitude of the acceleration of the two profiles is kept constant, then the twin pulse degenerates to a single boxcar (Figure 8).

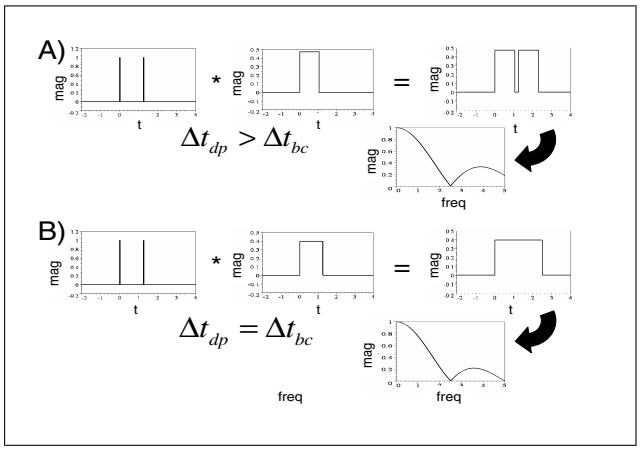

Fig. 8: *Comparison of when a twin pulse and boxcar degenerates to a single boxcar; A) Result of combining a twin pulse of width = $\Delta t_{TP} = 0.4\pi$ and a boxcar of width = $\Delta t_{BC} = 0.4\pi - 0.2$; B) Result of combining a twin pulse of width $\Delta t_{TP} = \Delta t_{BC} = 0.4\pi$.*

There is an advantage of using the boxcar kernel to generate profiles. The boxcar profile is the standard profile used in most commercial motion control systems. This profile is the first half of what is usually referred to as a trapezoidal velocity profile. Given the notch or natural frequency ω_n and the desired slew velocity v the acceleration command a can be computed for a ramp velocity profile.

$$\begin{array}{l} \omega_n = \frac{2\pi}{\Delta t} \\ v = a\ \Delta t \end{array} \tag{9}$$

Combine, eliminating Δt, and then solving for a results in.

$$a = \frac{v\ \omega_n}{2\pi} \tag{10}$$

The duration of the acceleration section of the profile is given by.

$$\Delta t_{(BC:VR)} = \frac{v}{a} = \frac{2\pi}{\omega_n} \tag{11}$$

E. Boxcar / Trapezoidal (BC:TZ) Swing-Free Profile

Even though the Boxcar / Velocity Ramp (BC:VR) kernel is easily implemented in most commercial motion control systems, the sensitivity of the narrow notch in the frequency spectrum makes the single boxcar profile impractical in most applications. The robustness can be improved by using the combining technique described in section III-C. The trapezoidal frequency spectrum (acceleration followed by a deceleration) can be combined with the boxcar frequency spectrum. If the desired profile starts at rest, slews a distance then comes to a stop (trapezoidal profile) the overall profile can be used to widen the notch in the frequency spectrum.

The trapezoidal profile can be broken down into two Dirac pulses (one positive and one negative) convolved with a boxcar function. As with the twin pulse and boxcar (TP:BC) example in section III-B, the null points in the frequency spectrum can be aligned to create the improved spectrum in Figure 9. In the twin pulse alignment technique the first null point of the twin pulse and boxcar spectrum were forced to align. In the BC:TZ profile the same technique is used but the null point must be picked to satisfy the distance and velocity constraints of a trapezoidal profile.

The distance and slew speed desired for the trapezoidal profile may require that the driven object cycles through many half cycles of its natural period before it is brought to rest. The first null frequency of the boxcar can still be used, but the fact that the system goes through many cycles requires that any null point of the trapezoidal pulse can be used. The first null point of the boxcar will be aligned with the trapezoidal null point that creates a slew velocity that comes closest to matching the desired slew velocity. In most cases, the null point will be picked that creates the largest velocity that does not exceed the desired slew velocity. The following are the governing equations for the null point alignment of a trapezoidal profile:

$$\begin{array}{lcl} t_{BC} & = & \frac{2\pi}{\omega_n} \\ t_{TZ} & = & \frac{2\pi}{\omega_n} k \\ t_{(BC:TZ)} & = & t_{BC} + t_{TZ} = \frac{2\pi(1+k)}{\omega_n} \\ v_{slew} & = & \frac{d}{t_{TZ}}, \end{array} \tag{12}$$

where

$$\begin{array}{ll} d & = \text{Distance to travel} \\ v_{slew} & = \text{Slew velocity of trapezoidal profile} \\ t_{BC} & = \text{Duration of boxcar} \\ t_{TZ} & = \text{Duration between trapezoidal pulses} \\ t_{BC:TZ} & = \text{Total time of trapezoidal profile} \\ k & = \text{Null point number of trapezoidal profile.} \end{array}$$

Equation (12) can be solved for k;

$$k = ceil\left(\frac{d\ \omega_n}{2\ \pi\ v_{slew}}\right). \tag{13}$$

When computing k the desired slew velocity (v_{slew}) is used. The value of k is then rounded up to the nearest integer. Once k is computed, the durations of the trapezoidal profile t_{TZ} and boxcar t_{BC}profile can be computed. Lastly the actual slew velocity for the profile is computed also using k,

$$v_{actual\ slew} = \frac{d\omega_n}{2\pi k}. \tag{14}$$

F. Mis-aligned Boxcar / Trapezoidal (M-BC:TZ) Swing-Free Profile

The mis-alignment technique used for the twin-pulse profile can also be used for the trapezoidal profile with the same widened-frequency spectrum notch. The results for such a profile can be seen in Figure 10. The formulation to compute the durations of trapezoidal pulses and boxcar profiles is similar to that for the aligned trapezoidal profile. Only the

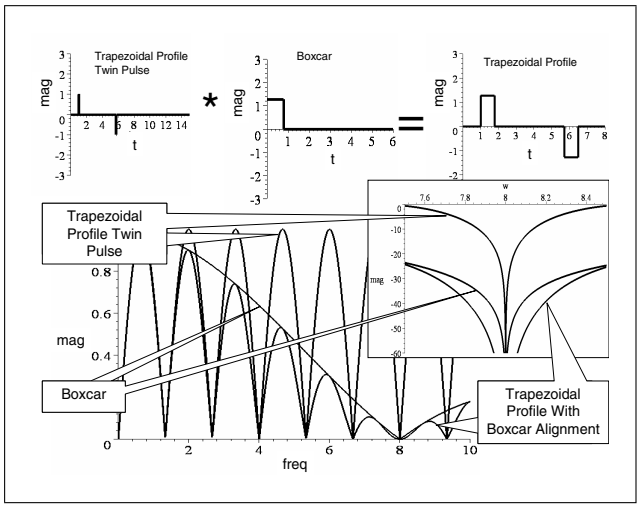

Fig. 9: *Trapezoidal profile with frequency spectrum of the pulses and boxcar aligned.*

offset $\delta\omega_n$ must be added and subtracted from the natural period of the system in (12).

$$\begin{aligned} t_{BC_{(M-BC:TZ)}} &= \frac{2\pi}{\omega_n - \delta\omega_n} \\ t_{TZ_{(M-BC:TZ)}} &= \frac{2\pi}{\omega_n + \delta\omega_n} k \\ t_{(M-BC:TZ)} &= t_{BC_{(M-BC:TZ)}} + t_{TZ_{(M-BC:TZ)}} \\ &= \frac{2\pi(\omega_n(k+1) - \delta\omega_n(k-1))}{\omega_n^2 - \delta\omega_n^2} \\ v_{slew} &= \frac{d}{t_{TZ_{(M-BC:TZ)}}} \end{aligned} \quad (15)$$

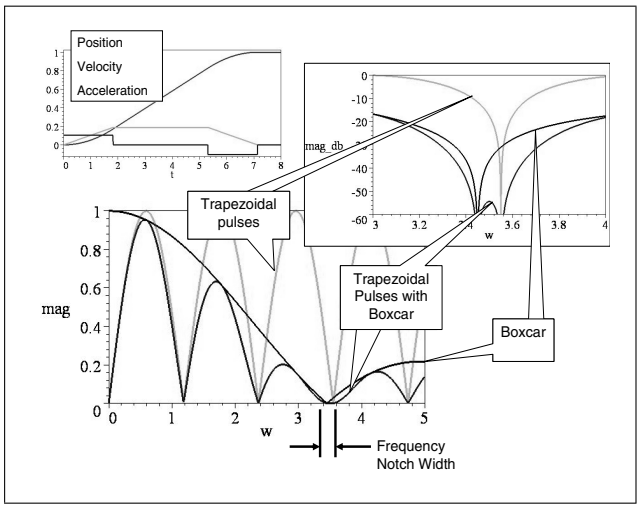

Fig. 10: *Trapezoidal profile with frequency spectrum of the pulses and boxcar slightly miss-aligned to increase width of frequency notch.*

As with the twin pulse mis-align technique, the $\delta\omega_n$ offset can be added to the trapezoidal ω_n and subtracted from the boxcar ω_n (referred to as the $M - BC : TZ$ method), or subtracted from the trapezoidal and added to the boxcar (referred to as the $M-BC:TZ$ method). The $M-TZ:BC$ method creates the profile with the shortest duration, but also has a larger magnitude, thus higher acceleration. The following are the governing equations for the null point mis-aligned trapezoidal profile:

$$\begin{aligned} t_{BC_{(M-TZ:BC)}} &= \frac{2\pi}{\omega_n + \delta\omega_n} n \\ t_{TZ_{(M-TZ:BC)}} &= \frac{2\pi}{\omega_n - \delta\omega_n} k \\ t_{(M-TZ:BC)} &= t_{BC_{(M-TZ:BC)}} + t_{TZ_{(M-TZ:BC)}} \\ &= \frac{2\pi(\omega_n(k+1) + \delta\omega_n(k-1))}{\omega_n^2 - \delta\omega_n^2} \\ v_{slew} &= \frac{d}{t_{TZ_{(M-TZ:BC)}}}. \end{aligned} \quad (16)$$

These equations can then be solved for k and the profile times computed:

$$k = ceil\left(\frac{d\,(\omega_n - \delta w)}{2\,\pi\,v_{slew}}\right). \quad (17)$$

When computing k the desired slew velocity (v_{slew}) is used. Once k is computed the actual slew velocity is computed using (16).

The frequency spectrum magnitude for the mis-aligned trapezoidal profiles is defined by (18). As with the mis-aligned, twin pulse profiles, the quantity $\delta\omega_n$ can be computed by iterating over the equations until the desired error is achieved at ω_n.

$$\begin{aligned} mag_{(M-BC:TZ)} = \Bigg| & \frac{j(\omega_n - \delta\omega_n)}{4\pi\omega_n} \\ & \left(e^{\left(\frac{-2j\pi\omega_n}{\omega_n - \delta\omega_n}\right)} + e^{\left(\frac{-2j\pi\omega_n k}{\omega_n + \delta\omega_n}\right)} - 1 \right. \\ & \left. - e^{\left(\frac{-2j\pi(\omega_n(k+1) - \delta\omega_n(k-1))}{\omega_n^2 + \delta\omega_n^2}\right)}\right)\Bigg| \end{aligned} \quad (18)$$

$$\begin{aligned} mag_{(M-TZ:BC)} = \Bigg| & \frac{j(\omega_n - \delta\omega_n)}{4\pi\omega_n} \\ & \left(e^{\left(\frac{-2j\pi\omega}{\omega_n + \delta\omega_n}\right)} + e^{\left(\frac{-2j\pi\omega k}{\omega_n - \delta\omega_n}\right)} - 1 \right. \\ & \left. - e^{\left(\frac{-2j\pi(\omega_n(k+1) + \delta\omega_n(k-1))}{\omega_n^2 + \delta\omega_n^2}\right)}\right)\Bigg| \end{aligned} \quad (19)$$

G. Mis-aligned Boxcar / Trapezoidal / Twin Pulse (M-BC:TZ:TP) Motion Profile

The mis-alignment technique can be taken one step further by combining the twin pulse, boxcar, and trapezoidal profiles together. When two base profiles are combined, two possible resulting profiles exist. When three base profiles are combined, six resulting profiles are possible. The number of resulting profiles can be reduced to two if the trapezoidal profile is always the center profile. This can be justified by viewing the frequency spectrum of the three profiles. The frequency spectrum of the trapezoidal profile will usually have the narrowest notch. This narrow notch is a result of the distance and time required to traverse the trapezoidal profile. For long duration moves, the system will go through many cycles. The more cycles required to traverse the profile, the more compact the lobes become in the frequency spectrum. This compaction of the spectrum creates narrow notches. For each complete cycle of the system there will be a null point to the left of

the desired notch frequency. This requires the alignment of high order null points with the first null points of the twin pulse and boxcar. Placement of the wider notches (slope of the frequency spectrum near the null point) of the twin pulse and boxcar profiles on each side of the trapezoidal profile helps to increase the overall width of the notch.

The triple mis-alignment technique can be thought of as the twin pulse boxcar technique described above with the trapezoidal profile centered at the notch frequency. The kernel length of the triple mis-alignment is then the length of the TP:BC profile (equations (7) and (8)) with the duration of the trapezoidal profile added.

$$t_{(\mathrm{M-BC:TZ:TP})} = \frac{\pi(3\omega_n - \delta\omega)}{\omega_n^2 - \delta w^2} + \frac{2\pi k}{\omega_n} \tag{20}$$

$$t_{(\mathrm{M-TP:TZ:BC})} = \frac{\pi(3\omega_n + \delta\omega)}{\omega_n^2 - \delta w^2} + \frac{2\pi k}{\omega_n} \tag{21}$$

The frequency spectrum magnitude for the TP:TZ:BC profiles is defined by (22). As with the mis-aligned boxcar, twin pulse and mis-aligned boxcar trapezoidal profiles, a $\delta\omega_n$ offset can be computed by iterating over the equations until the desired error at ω_n is achieved:

$$\begin{aligned} mag_{(M-TP:TZ:BC)} \quad = \quad & \left| \frac{j(\omega_n+\delta\omega_n)}{4\omega\pi} \left(e^{\left(\frac{-j\pi\omega_n}{\delta\omega_n-\omega_n}\right)} + 1 \right) \right. \\ & \left(e^{\left(\frac{-2j\pi\omega_n}{\omega_n+\delta\omega_n}\right)} - 1 \right) \\ & \left. \left(1 - e^{\left(\frac{-2j\pi\omega_n}{\delta\omega_n-\omega_n}k\right)} \right) \right|, \end{aligned} \tag{22}$$

$$\begin{aligned} mag_{(M-BC:TZ:TP)} \quad = \quad & \left| \frac{j(\omega_n+\delta\omega_n)}{4\omega\pi} \left(e^{\left(\frac{-j\pi\omega}{\delta\omega_n-\omega_n}\right)} + 1 \right) \right. \\ & \left(e^{\left(\frac{-2j\pi\omega}{\omega_n-\delta\omega_n}\right)} - 1 \right) \\ & \left. \left(1 - e^{\left(\frac{-2j\pi\omega}{\delta\omega_n+\omega_n}k\right)} \right) \right|. \end{aligned} \tag{23}$$

Figure 11 is a comparison of a M-TP:BC profile with a M-TP:TZ:BC profile with the same $\delta\omega_n$ offset. In this comparison we see that the addition of the trapezoidal spectrum reduces the response by over 10db. The effect of the triple mis-alignment profile can be thought of as two filters in series, reducing the residual vibrations in a sequential fashion.

The example spectra in Figure 11(A) shows a TP:BC profile and a M-TP:TZ:BC profile. During the ramp-up acceleration phase of the profile, only the TP:BC portion of the profile is felt by the system. At this point in the profile the residual vibration will attenuated by 48db. During the ramp-down deceleration phase of the profile, the resedal vibration will be attenuated an extra 12db to 60db due to the added alignment of the trapezoidal part of the profile. Figure 11 also shows the difference of the a M-TP:BC profile and a M-TP:TZ:BC profile with $\delta\omega_n$ offsets adjusted to create the same magnitude of filtering at the frequency notch.

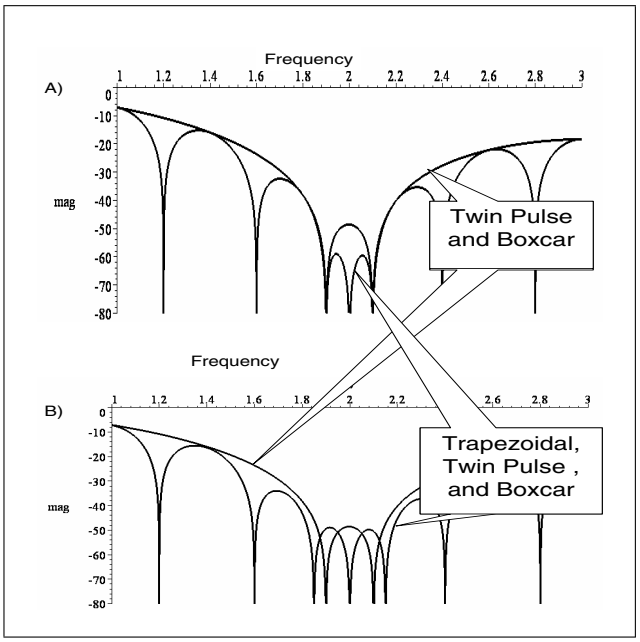

Fig. 11: *A) Mis-aligned twin pulse with boxcar (M-TP:BC) frequency spectrum compared to twin pulse with boxcar and trapezoidal (M-TP:TZ:BC) with equal $\delta\omega$'s; B) Mis-aligned twin pulse with boxcar (M-TP:BC) frequency spectrum compared to twin pulse with boxcar and trapezoidal (M-TP:TZ:BC) with $\delta\omega$'s adjusted to create equal magnitude attenuated.*

IV. Experimental Results

An experiment was conducted using a multi-pendulum device. The lengths of the 10 pendula were arranged to have a frequency span of 3.36 rad/s to 3.66 rad/s. The frequency range corresponds to a the masses on the pendula being being evenly spaced between 28.8 in to 34.2 in.

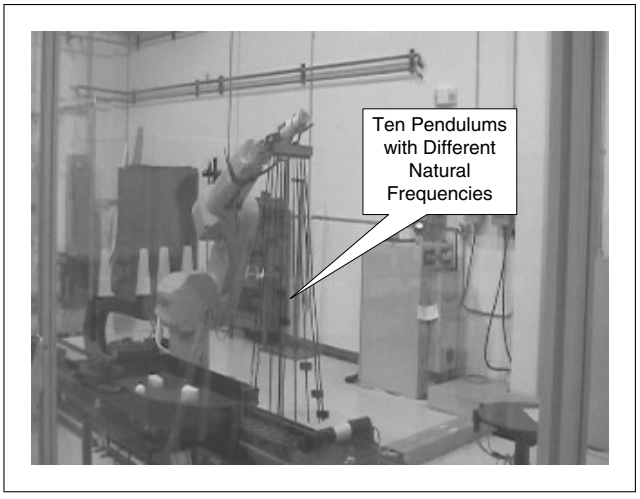

Fig. 12: *Multiple pendula of different lengths (the comb) being driven at the University of New Mexico by the RTU in the MTTC robotics lab.*

The pendula were driven a distance of 1.7 meters using two different profiles. The first profile was a classic twin pulse profile with a slew velocity of 0.7 m/s shown in Figure 13.

The second profile was an expanded twin pulse (M-BC:TZ:TP) motion profile with a desired slew velocity of 0.7 m/s which resulted in an actual velocity (see Equation 16, k=2) of 0.4735 m/s (Figure 14). The pulses in both profiles were constructed using Boxcar filters such that the area under the Boxcars (acceleration profile) was equal to the slew velocities. Both profiles were constructed to have frequency notches centered at 3.5 rad/s. The (M-BC:TZ:TP) profile was designed with a δw_n of 0.05 rad/s above and below the notch frequency. From Figures 13 and 14 it can be seen that the acceleration profiles of both methods have the same form. But by using the methods presented herein the narrow notch of the classic twin pulse profile has been significantly widened around 3.5 rad/s.

Both profiles were initially tested on a simulation of the pendula. The results of the simulations are shown in Figure 15. From the figure it can be seen that the (M-BC:TZ:TP) profile eliminated virtually all residual vibrations over the frequency range of the pendula, while the classic twin pulse profile only eliminated the residual vibration of the pendula near 3.5 rad/s.

The simulation showed a reduction in residual oscillations of 97% using the (M-BC:TZ:TP) profile as compared to the classic twin pulse profile for the natural frequency range of the pendula used in the simulation (of 3.36 rad/s to 3.66 rad/s). The classic twin-pulse profile produced a maximum oscillation of 0.374 degs whereas the the (M-BC:TZ:TP) profile had a maximum oscillations of 0.012 degs.

When the actual pendula were driven with the profiles in Figures 13 and 14, the results matched that of the numerical simulations. When the classic twin pulse system came to rest only one of the pendula had virtually no residual oscillations while the remaining pendula had a noticeable motion. The experiment also showed the sensitivity of unexpanded twin pulse profiles. The profile was created based on a computed ω_n=3.5 rad/s for the center pendulum. The pendulum that came to rest was the shortest pendulum which had a computed natural frequency of 3.66 rad/s.

This offset of the twin pulse frequency notch is also apparent in the frequency spectrum of Figure 13. The notch in the spectrum is not exactly at 3.5 rad/s. The spectrum in the figure was created from the actual profile used in the experiment. The linear rail transport system used to drive the pendula has a position-time update resolution of $1/60$ second. The time required for a twin pulse to notch out 3.5 rad/s (see Equation 3, $k = 1$) is $\pi/\omega_n = \pi/3.5 = 0.8976$ which is not evenly divisible by $1/60$ contributing to the sensitivity of implementing twin pulse profiles.

The expanded twin pulse (M-BC:TZ:TP) experiment closely matched the numerical simulation without any sensitivity issues. When the (M-BC:TZ:TP) system came to rest all of the pendula came to rest with virtually no residual oscillations.

V. Conclusion

This paper demonstrates how the original swing free twin pulse profile can be modified to increase significantly its robustness. The method is based on exploiting the frequency response of all the components used to construct a twin pulse profile. The technique includes intentionally mis-aligning the null points of ideal twin pulses and a convolved boxcar function, then adding a trapezoidal profile component, finally culminating in what we term a "mis-aligned boxcar / trapezoidal / twin pulse" (M-BC:TZ:TP) motion profile.

This expanded profile and a basic twin-pulse profile were both evaluated on a ten-pendula system with natural frequencies from 3.36 to 3.66 rad/s. Simulation of the profiles showed a reduction in residual oscillations of 97% using the (M-BC:TZ:TP) profile as compared to the classic twin pulse pro-

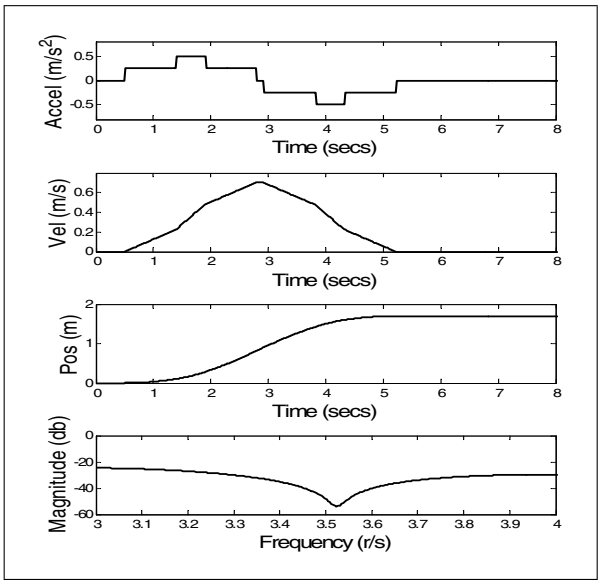

Fig. 13: *Acceleration, velocity, position, and frequency response of classic swing free (twin pulse) profile.*

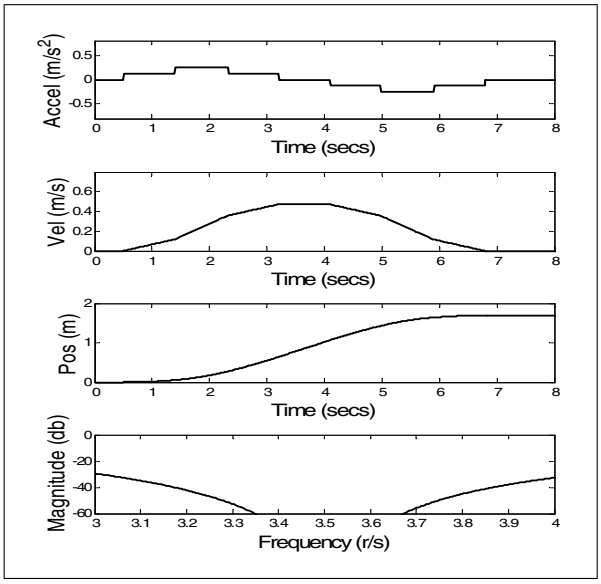

Fig. 14: *Acceleration, velocity, position, and frequency response of Mis-aligned Boxcar / Trapezoidal / Twin Pulse (M-BC:TZ:TP) motion profile.*

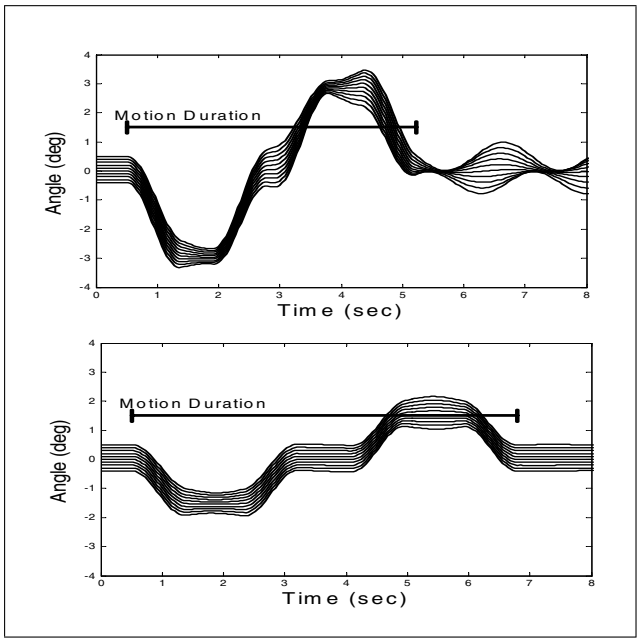

Fig. 15: *Comparison of results of simulated classic swing free (twin pulse) profile (upper plot) and expanded twin pulse (M-BC:TZ:TP) Motion Profile (lower plot). Both plots show the swing angles of each of the 10 pendula of the comb in Figure 12. The lengths of the 10 pendula were arranged to have a frequency span of 3.36 rad/s to 3.66 rad/s.*

file. Experiments using a linear rail transport system and the ten-pendula device validated the techniques. These expanded profiles retain the simplicity and short duration of the twin-pulse with increased robustness to frequency variations.

VI. Acknowledgement

We'd like to thank Dave Vick for his help in the experimental validation of the classic and expanded twin pulse profiles.

References

[1] Smith O. J. M., *Posicast Control of Damped Oscillatory Systems* Proceeding of the IRE, September 1957, pg 1249-1255

[2] Tallman G.H., Smith O. J. M. *Analog Study of Dead-Beat Posicast Control* IRE Transactions of Automatic Control, March 1958, pg 14-21

[3] Starr, P, G. *Swing-free transport of suspended objects with a path controller robot manipulator*, ASME Journal of Dynamics Systems Measurement and control, March 1985, vol 107, pg 97-100

[4] Bowling D., Starr G., Wood J., Lumia R. *Wide Band Suppression of Motion-Induced Vibration*, IEEE International Conference on Robotics and Automation, 2007

[5] Khalsa, S, Dharam *High Performance Motion Control Trajectory Commands Based On The Convolution Integral and Digital Filtering*, PCIM Intelligent Motion Conference, October 1990, pg 54-64

[6] Gursel A., Sadettin K., and Sedat B. *Swing-free transportation of suspended objects with robot manipulators*, Robotica, 1999, vol 17, pg 513-521

[7] Singer, N., and Seering W., *Preshaping Command Inputs to Reduce System Vibration*, ASME Journal of Dynamics Systems Measurement and control, March 1990, vol 112, pg 76-82

[8] Singhose, W., Derezinski, S., Singer, N. *Input Shapers for Improving the Throughput of Torque-Limited Systems*, Proceeding of the 1994 Conference on Control Applications, 1994

[9] Singhose, W., Singer, N. *Initial Investigations into the Effect of Input Shaping on Trajectory Following* , Proceeding of the 1994 American Control Conference, 1994

[10] Singhose, W., Bohlke, K., Seering, W. *Fuel-Efficient Shaped Command Profiles for Flexible Spacecraft*, Proceeding of the 1995 AIAA Guidance, Navigation, and Control Conference, 1995

[11] Singhose, W., Seering, W., Singer, N. *The Effect of Input Shaping on Coordinate Measuring Machine Repeatability*, Proceeding of the 1995 IFToMM World Congress on the Theory of Machines and Mechanisms, 1995

[12] Singhose, W.,Chuang T. *Reducing Deviations from Trajectory Components with Input Shaping*, 1995 American Control Conference, 1995

[13] Singhose, W., Singer, N. , Seering, W.*Comparison of Command Shaping Methods for Reducing Residual Vibration*, Proceedings of the 1995 European Control COnference, 1995

[14] Pao, L., Singhose, W.*Unity -Magnitude Input Shapers and their Relation to Time-Optimal Control*, Proceeding of the 1996 IFToMM World Congress, 1996

[15] Crain, E., Singhose W., Seering*Derivation and Properties of Convolved and Simultaneous Two-Mode Input Shapers*, Proceeding of the 1996 IFToMM World Congress, 1996

[16] Singhose W., Crain, E., Seering *Convolved and Simultaneous Two-Mode Input Shapers*, IEE Proceeding of Control Theory and Applications, Nov 1997, vol 144 No 6, pg 515-520

[17] Singhose W., Porter, L., Tuttle, T., Seering*Vibration Reduction Using Multi-Hump Input Shapers*, Transactions of the ASME, June 1997, vol 119, 1997, pg 320-326

[18] Pao, L., Lau, M. *Input Shaping Design to Account for Uncertainty in Both Frequency and Damping in Flexible Structures*, Proceeding of the American Control Conference, Philadelphia, PA, June 1998

[19] Economou, D., Mavroidis, C., Antoniadis, I.*Robust vibration suppression in flexible systems using infinite impulse response digital filters* Journal of Guidance, Control, and Dynamics (0731-5090) 2004 vol. 27 no. 1

[20] Economou, D, Mavroidis, C, Antoniadis, I, Lee, C *Maximally robust input residual preconditioning for residual vibration suppression using low-pass FIR digital filters* Journal Of Dynamic Systems Measurement And Control-Transactions of The ASME; Mar 2002, V.124, No.1, P.85-97

[21] Glossiotis, G. N., Antoniadis, I. A. *Digital Filter Based Maximally Robust and Time Optimal Vibration Free Motion Structures with Densely Pack Modes*

[22] Craig, J., John *Introduction to Robotics Mechanics and Control*

[23] Smith W., Steven *Digital Signal Processing*, 2003

[24] Lyons G. Richard *Understanding Digital Signal Processing*, 2004

[25] James M.L., Smith G.M., Wolford J.C *Applied Numerical Methods for Digital Computation*, 1985

[26] Oppenheim, Alan and Schafer, Ronald *Discrete-Time Signal Processing, Second Edition*, 1999

[27] Bracewell, Ronald *The Fourier Transform and its Application*, 2000